Effect of Acetic Acid and/or Sodium Hydroxide Treatment towards Characters of Wonosari Natural Zeolite for Hydrotreatment of Castor Oil into Biofuel

Triyono Triyono, Wega Trisunaryanti*, Iip Izul Falah, and Lailatul Rahmi

Department of Chemistry, Faculty of Mathematics and Natural Sciences, Universitas Gadjah Mada, Sekip Utara, Yogyakarta 55281, Indonesia

* Corresponding author:

tel: +62-811256055
email: wegats@ugm.ac.id

Abstract: *Natural zeolite (ZA) obtained from Wonosari, Indonesia, was treated with acetic acid (ZAA) or NaOH (ZAB), and the combination of both treatments (ZAAB) in order to increase the Si/Al ratio and catalytic performance on hydrotreatment of castor oil. The Si/Al ratio of ZA increased after the combination of acetic acid and NaOH treatment. The change of the Si/Al ratio was observed in the FTIR spectra as the shifting of internal asymmetric stretching vibration of T–O–T at 1032-1100 cm^{-1}. The XRD profile of ZA was maintained after being subjected to treatments, and ZAB exhibited the lowest crystallinity. The surface area of the ZA after treatment is in the order ZAA < ZA < ZAAB < ZAB. The ZAB catalyst having the highest surface area (19.144 m^2 g^{-1}) showed the highest catalytic activity on the hydrotreatment of castor oil with a liquid fraction of 55.1 wt.% and selectivity towards the hydrocarbon compounds of 22.40 wt.%.*

***Keywords:** acetic acid; natural zeolite; sodium hydroxide; hydrotreatment*

■ INTRODUCTION

The usage of fossil fuels presents two significant difficulties. The first is its quick decline in value and rising prices. The second is its environmental impact due to the toxic gases (CO_X, SO_X, and NO_X) created during the combustion of conventional fuels and other air pollutants. These led to various negative environmental, ecosystem, human health consequences, and their significant contribution to the greenhouse effect [1]. As a result, numerous researchers have begun investigating alternative energy sources with manageable environmental implications. Biofuel was once regarded as one of the considerable substitutes for conventional diesel fuel [2]. Biofuel is a non-toxic, environmentally benign, and biodegradable fuel [3]. Furthermore, it is compatible with current engines without modification [4].

Non-edible biofuel feedstocks are receiving global attention due to their widespread distribution. Additionally, they can alleviate food competition, are environmentally friendly, provide valuable products (glycerol), and are more cost-effective as a feedstock than edible oils [5]. Second-generation biodiesel is considered to be oil derived from non-edible plants. Some of the potential non-edible oil-producing plants are *Jatropha curcas* L. (jatropha), *Thespesia populnea* L. (milo), *Pongamia pinnata* (Karanja or honge), *Moringa oleifera* (drumstick tree), *Calophyllum inophyllum* L. (undi), *Croton megalocarpus* (croton), and *Ricinus communis* L. (castor) [6].

Natural zeolites are utilized in a variety of processes that result in the production of chemicals, fuels, and other commodities. Designing zeolite catalysts with better selectivity, lower operating temperatures, and increased stability is vital. Optimizing the porosity structure in enhanced zeolite catalysts enhances mass transfer and active site design. Sites that are unattractive and take away from the benefits of active sites must be eliminated or prohibited [7]. On the other hand, natural zeolite requires a precise acid and alkali treatment to maintain the silicon-aluminum ratio and specific surface area [8].

Acid treatments, in general, can remove impurities such as SiO_2, Al_2O_3, and Fe_2O_3 from the zeolite's surface and pores. Simultaneously, the acid solution dissolves amorphous materials within the pores and exchanges

large cations for small protons via ion exchange, increasing the pore size, specific surface area, and adsorption capacity. Additionally, acid treatment modifies the surface properties of the zeolite molecular sieve, optimizing the mordenite material's qualities. Meanwhile, alkali treatment is a widely used technique for partially dissolving the zeolite structure due to silicon extraction. At a somewhat higher reaction temperature, catalytic cracking might be employed to get a high yield of hydrocarbon biofuel from vegetable oil [9-10]. Catalytic cracking is a simple and cost-effective method of converting vegetable oil to hydrocarbon biofuel [11].

One option to use the higher biofuel content in diesel fuel is to use hydrotreated vegetable oils. This would provide another way to accomplish our CO_2 reduction goal in the future [12]. There may be economic implications associated with efforts to reduce environmental pollution. Economic growth and carbon emissions are positively related, which indicates that reducing emissions could hinder economic growth. Additionally, pollution control measures may require increased production costs, which could also slow economic growth. Biofuels are renewable in comparison to fossil fuels. The topic of biofuels is still in its early stages in terms of technological progress [13].

Hydrotreating and hydrotreatment are both examples of hydroprocessing. Because it eliminates heteroatoms and saturates C–C bonds while retaining carbon atom count, hydrotreating is preferred for diesel range fuel. Hydrocracking (a severe form of hydroprocessing) induces the breakdown of C–C bonds to produce gasoline-range fuels [14]. Hydroprocessing is a procedure that is frequently used in refineries and vegetable oil upgrading to remove oxygen via the addition of H_2 [15]. The choice of a hydrotreating catalyst is essential in determining the yield and quality of hydrotreating products. Hydrotreating catalysts are often composed of essential metals such as Mo, Co, and Ni as active metals and are supported by alumina or silica-alumina [16]. Kristiani et al. [17] reported converting ethanol to gasoline utilizing a natural catalyst supported by different transition metals, including Ni, Co, Cu, and Zn. Their catalytic activity was evaluated for ethanol to

gasoline conversion and demonstrated a high conversion rate of up to 80–90%. The addition of Ni, Ni-Mo, Co, and Co-Mo metals was loaded into the activated natural zeolite to increase the activity and selectivity for the hydrocracking process [18]. As Sun et al. [19] stated, the development of zeolite-supported metal catalysts has promoted the progress of heterogeneous catalysis, which exhibited excellent performance in much catalytic activity.

Numerous studies have employed catalysts impregnated with metals. However, these metals can be wasteful and expensive. Additionally, impregnation of the metal might result in blockage (closing of pores), resulting in lower catalytic activity. Typically for zeolite treatment by employing a strong acid such as (HCl, HNO_3, and H_2SO_4), as performed by Trisunaryanti et al. [20], mordenite's Si/Al ratio increased as a result of HNO_3 acid treatment, and the treatments did not cause damage to the crystalline structure of the mordenite.

Another study by Anggoro et al. [21] employed the strong acid H_2SO_4 to treat zeolite Y. However, the treatment using strong acid is not environmentally friendly. As a result, this research employs acetic acid, a more environmentally friendly organic acid, as previously done by Chung [22]. In this research, the natural zeolite was treated with acetic acid and sodium hydroxide to improve the natural zeolite character.

Base treatment with NaOH is the common method applied to zeolite treatment [23]. Base treatment of zeolites with intermediate Al contents involves the selective extraction of silicon atoms resulting in a decrease of the Si/Al ratio or increase (case of low Si/Al ratio) and a significant loss of material at high base concentration [24]. Numerous investigations have demonstrated that activating natural zeolites with NaOH can increase crystallinity and the Si/Al ratio in catalysts at low concentrations such as 0.2 M [25]. The presence of the weak, medium and strong acid sites in zeolite altered the Si/Al ratio, which depends on the NaOH solution concentration and the zeolite composition [26]. The originality of this research is the treatment of natural zeolite with a weak organic acid (acetic acid) and base treatments (sodium hydroxide),

which has not been conducted previously and extensively. The catalyst activity in hydrotreatment with castor oil was then determined.

■ EXPERIMENTAL SECTION

Materials

Natural zeolite was obtained from Wonosari, Yogyakarta Special Region, Indonesia. The glacial acetic acid (CH_3COOH), sodium hydroxide (NaOH), Whatman filter paper No. 42, and universal pH paper were acquired from Merck. Co. Castor oil was purchased from CV Fruitanol Yogyakarta. The distilled and demineralized water was supplied by CV. Progo Mulyo. While the H_2, and N_2 gas were supplied from PT. Samator Gas Industri.

Instrumentation

The metal contents in the zeolite samples were characterized using X-Ray Fluorescence (XRF, RIGAKU-NEXQC+QuanTEZ). The change in the Si-O-Al functional group was determined using Fourier-Transform Infrared spectrometer (FTIR, Thermo Nicolet Avatar 360 IR) at the wavenumber range of 400–4000 cm^{-1} using KBr pellet. X-Ray Diffraction (XRD, D2 Phaser diffractometer) using monochromatic Cu Kα source with a 2θ scan range of 3–80° and a scan speed of 3°/min. A surface Area Analyzer (SAA, JWGB meso 112) was conducted to obtain the porosity properties of the samples. The liquid product was analyzed using Gas Chromatography-Mass Spectrometry (GC-MS, Shimadzu QP2010S).

Procedure

Acetic acid treatment on natural zeolite (ZA)

Natural zeolite (denoted as ZA) was heated under stirring in 6 M CH_3COOH solution (ZA: acetic acid ratio of 1:5 (w/v)) for 10 h at 75–80 °C. Afterward, the mixture was filtered and washed using aquadest until pH neutral was achieved and dried at 110 °C for overnight to obtain ZAA. The ZA and ZAA were characterized using XRF, XRD, FTIR, and SAA.

Sodium hydroxide treatment on ZA and ZAA

ZA was heated under stirring in 0.1 M NaOH solution with ZA volume ratio towards sodium hydroxide of 1:5 at 75 °C for 30 min, continued with aging for 30 min.

The mixture was then washed by aquadest until neutral and dried at 110 °C for 24 h, to produce ZAB. The ZAA was also treated using the same procedure as mentioned to obtain ZAAB. The ZAB and ZAAB were characterized using XRF, XRD, FTIR, and SAA.

Catalytic activity test of catalysts

The catalytic activity of catalysts (ZA, ZAA, ZAB, and ZAAB) was tested on the hydrotreatment process of castor oil. A sufficient amount of catalyst and feed was put into a bed in a stainless steel reactor (i.d = 2.0 cm, o.d = 2.2 cm, l = 30 cm). The catalyst/feed weight ratio was 1/100 wt.%. The hydrotreatment process was carried out at 450 °C for 2 h under H_2 gas with a flow rate of 10 mL/min. The product obtained from the reaction was flown into a condenser, where it was allowed to cool down using an ice bath in a flask. The percentage (%) of each product yield was determined gravimetrically using Eq. (1-3).

$$\text{Liquid product (wt.\%)} = \frac{\text{weight of liquid product}}{\text{weight of initial feed}} \times 100\% \quad (1)$$

$$\text{Coke (\%)} = \frac{\text{Catalyst weight differences before and after reaction}}{\text{weight of initial feed}} \times 100\% \quad (2)$$

$$\text{Residue (wt.\%)} = \frac{\text{Weight of remained feed}^*}{\text{weight of initial feed}} \times 100\% \quad (3)$$

$$^* = W_1 - W_0$$

where, W_0 = the weight of empty feed part, W_1 = the weight of the feed part after the catalytic process.

$$\text{Total conversion (wt.\%)} = 100 - \text{residue (wt.\%)} \quad (4)$$

The liquid products were analyzed by using GC-MS to determine gasoline and diesel fraction. Gasoline fraction was hydrocarbon compounds consisting of carbon numbers between C_4 to C_{12}, while diesel fraction consisted of those with hydrocarbon chains between C_{13} to C_{22}. The selectivity of these products was calculated by using Eq. (5-7).

$$\text{Gasoline fraction (wt.\%)} = \frac{\text{Area GC of } C_4 \text{ to } C_{12} \text{ compounds}}{\text{Total area GC}} \times \text{Liquid product (wt.\%)} \quad (5)$$

$$\text{Diesel fraction (wt.\%)} = \frac{\text{Area GC of } C_{13} \text{ to } C_{22} \text{ compounds}}{\text{Total area GC}} \times \text{Liquid product (wt.\%)} \quad (6)$$

$$\text{Other compounds (wt.\%)} = \frac{\text{Area GC of nonhydrocarbon compounds}}{\text{Total area GC}} \times \text{Liquid product (wt.\%)} \quad (7)$$

■ RESULTS AND DISCUSSION

The Effect of Acetic Acid and NaOH Treatment towards Characters of Zeolite

Table 1 shows the results of the XRF analysis, which revealed that the ZA contains metal impurities such as Ca 5.80% and Fe 5.01%. Following acetic acid treatment, contaminants were still present and slightly increased; this could have occurred as a result of the dealumination process, which also removed some of the contaminants. The dealumination process removed metal contaminants such as Ca and Fe and removed Al, which was further proved by the slight increase in the Si/Al ratio from 7.30 to 7.85 for the ZA and ZAA, respectively. This result confirmed that the acetic acid successfully removed aluminum atoms, as previously reported by others [22,27]. The breakage of Al caused the removal of Al–O bonds which were more accessible than the Si–O bonds, whereas the dissociation energy of the Al–O bond (116 kcal/mol) is lower than the Si–O bond (190 kcal/mol). Notably, the Si/Al ratio change after acetic acid treatment was insignificant because acetic acid is weak. The strength of acetic acid can be seen from its dissociation constant, which has a Ka value of 1.7×10^{-5}. The greater the Ka value, the easier CH_3COO^- and H^+ to dissociate. In this case, the CH_3COO^-'s ability to bind to Al^{3+} was not strong, which caused the removal of non-framework aluminum atoms rather than the Al framework (FAL). When aluminum is removed, the zeolite structure is frequently disrupted, resulting in octahedral coordinated extra framework aluminum (EFAL) within the pores [28]. The dealumination process begins with the cleavage of O–Al–O bonds, then the atoms leave atomic gaps, and silanol nests and refills empty spaces by Si atoms.

The ZA and ZAB have the content of silicon which slightly decreased from 77.41 to 68.56, and for ZAA and ZAAB, 77.09 to 74.64. This result proved that NaOH treatment successfully removed the silicon content from the framework. However, it is noticeable that Si/Al ratio slightly changes even after the NaOH treatment (ZAB and ZAAB samples), and the result is not greater than 25. This finding suggests that some aluminum content might also

Table 1. Metal compositions and Si/Al ratio of zeolite

Compositions (%)	ZA	ZAA	ZAB	ZAAB
Al	10.5	9.82	9.43	9.79
Si	77.4	77.0	68.5	74.6
Ca	5.80	6.58	8.95	8.29
Fe	5.01	5.27	7.60	5.74
Ni	0.07	0.09	0.13	0.11
Cu	0.04	0.04	0.06	0.06
Zn	0.03	0.04	0.07	0.06
Si/Al Ratio	7.30	7.85	7.26	7.61

remove from the framework during NaOH treatment. The silicon and aluminum are close when the Si/Al ratio is low. Aluminum is removed along with silicon due to aluminum's amphoteric properties [29].

FTIR Characterization

Zeolite materials incorporate the network between tetrahedral $[SiO_4]^{2-}$ and $[AlO_4]^{5-}$, which are detectable in the FTIR characterization's energy range. Moreover, the FTIR characterization could be employed to identify the Brønsted and Lewis acid sites that arise from the natural zeolite and its modification. Overall, the bands observed in the range of 445–464 cm^{-1} indicate the bending vibration of T–O–T groups (T = Si or Al atoms) in the zeolite. The vibration of T–O–T groups also appears at a wavenumber of 794 cm^{-1} attributing to the symmetric stretching vibration. The bands around 1032–1100 cm^{-1} assigned to the internal asymmetric stretching vibration of T–O–T groups could be used to observe the change in the Si/Al ratio of zeolite due to the continued removal of aluminum and silicon's removal [30]. Additionally, the bands assigned to the OH groups attached to the Al or Si observe at 3451–3457 and 3600–3650 cm^{-1}.

Fig. 1 presents the FTIR spectra of the natural zeolite before and after being subjected to the acid and NaOH treatment. The significant change after both treatments is the Si/Al ratio of zeolites observed in the FTIR as the shifting of the internal asymmetric stretching vibration of T–O–T. Fig. 1 observed that the bands at 1032–1100 cm^{-1} shifted, indicating the change in the Si/Al ratio of ZA after the acid and NaOH treatment. The acid treatment caused the bands to change
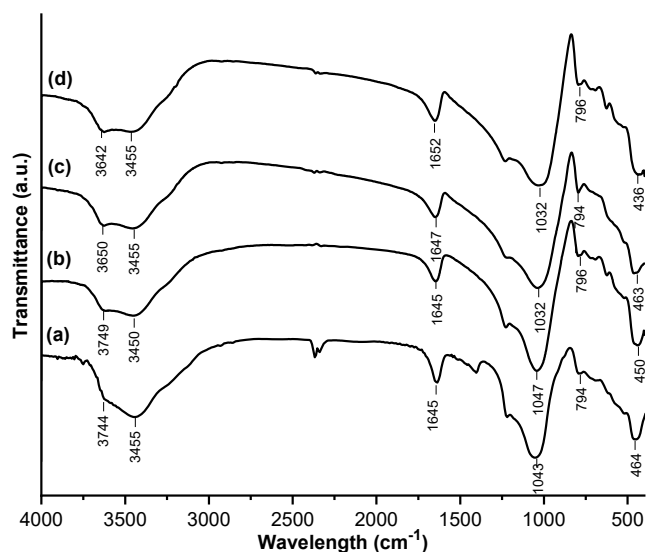
Fig 1. FTIR spectra of natural zeolite after the acid and NaOH treatment: (a) ZA, (b) ZAA, (c) ZAB, and (d) ZAAB

to a higher wavenumber from 1043 to 1047 cm^{-1}, contributing to the increasing Si/Al ratio. On the other hand, the NaOH treatment on both ZA and ZAA induced the shifting of internal asymmetric stretching vibration of T−O−T to lower wavenumber from 1043 to 1032 cm^{-1} and from 1047 to 1032 cm^{-1}, respectively. This result further validated that the NaOH treatment decreased the Si/Al ratio of zeolite.

The Effect of Acetic Acid and NaOH on Crystallinity

Natural zeolite usually contains many natural zeolites, such as Analcime, Clinoptilolite, Faujasite, Mordenite, and many more, which are greatly influenced

by zeolite's origin. Therefore, XRD characterization is needed to determine the kind of zeolite presented in the natural zeolite. Fig. 2(a) depicts the XRD profile of natural zeolite (ZA) obtained from Wonosari, Special Region of Yogyakarta, Indonesia. The XRD profile of the ZA indicated that it consists of mordenite and clinoptilolite as its primary structure. The mordenite peaks appeared at 2θ of 13.48°, 19.62°, 22.26°, 25.68, 26.24°, 27.62°, and 30.9° (JCPDS: 068448) and clinoptilolite profile presented at 2θ of 11.14°, 14.92°, 20.41°, 23.16°, and 32.15° (JCPDS: 251349). This result is in good agreement with the previous report on the use of zeolite obtained from the Special Region of Yogyakarta and the surrounding area [31-32]. Table 1 provides the chemical analysis by using XRF. It is noticed that ZA contains impurities atoms such as Fe, Ni, Cu, and Zn with a total of 5.15%. These atoms originated from the impurities mineral in ZA, such as pyrite (FeS$_2$). Other impurities compound found in the ZA is Albite (NaAlSiO$_3$), quartz (SiO$_2$), gibbsite (Al(OH)$_3$), and muscovite (KAl$_2$Si$_3$O$_{10}$(OH)$_2$) with a total composition of less than 20%.

Employing acetic acid in the dealumination preserve the crystallinity of the treated zeolite [22,27]. It can be clearly observed that after the treatment using acetic acid, the intensity of some peaks in the ZAA (Fig. 1(b)) increased, explaining that acetic acid treatment not only eliminates the aluminum atoms but also eliminates some impurities. On the other hand, NaOH treatment on
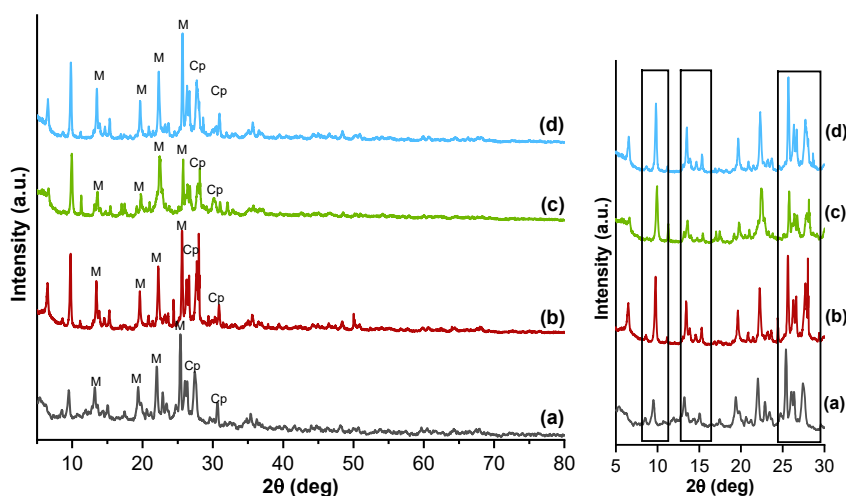
Fig 2. XRD spectra of (a) ZA, (b) ZAA, (c) ZAB, and (d) ZAAB (M = Mordenite, Cp = Clinoptilolite)

the ZA to obtain ZAB (Fig. 1(c)) caused a decrease in the crystallinity of Zeolite. It assumed that NaOH not only removes the silicon atoms but also aluminum atoms from the zeolite framework. It was proved by the ZAB's Si/Al ratio, which did not change much after the alkaline treatment (Table 1). The combination of the acid-alkaline treatment on the ZA (ZAAB) did not cause a significant decrease in the crystallinity of zeolite (Fig. 1(d)).

Adsorption Isotherm Curve

Fig. 3 shows the adsorption isotherm plot of the ZA before and after acid-alkaline treatment (ZAA, ZAB, and ZAAB). This type of plot can be considered a type IV isotherm typical for mesoporous materials, which have flat slits between two crystalline planes. The ZA is naturally a mesoporous material based on the isotherm plot and porous properties listed in Table 2. As shown in Fig. 3, even after the acid-alkaline treatment on ZA, the hysteresis type of treated ZA did not change. As indicated by the Si/Al ratio of the treated ZA (see Table 1), it suggested that the treatment condition is suitable for modifying the Si/Al ratio while maintaining the other properties. These phenomena are also supported by the XRD profile of ZAA, ZAB, and ZAAB, which have not significantly changed. Notably, from Fig. 3, the ZAA has low-pressure hysteresis while maintaining the hysteresis type. It may indicate the increased complexity of zeolite channels after acid treatment.

Fig. 4 present the range of pore distribution of zeolites between 2–20 nm, indicating that the pore ranges from the material were mesoporous. The specific surface area was determined on a sorption analyzer using the BET method. The specific surface area was determined to see the improved character of the catalysts after the zeolite was treated by acid and alkaline as well as metals impregnation, the sizes of pores can influence the order and the energy of activation of the catalytic reaction, and so it is essential to know the total specific surface area and the total pore volume are distributed in pores of the catalysts [33].

Table 2 lists zeolites' surface area, pore volume, and diameter change after acid-alkaline treatment. Interestingly, the surface area and total pore volume of ZA

after acid treatment (ZAA) decreased greatly from 12.542 to 4.058 $m^2 g^{-1}$ and 0.06 to 0.04 $cm^3 g^{-1}$, respectively. During the acetic acid treatment, the acetic acid disrupts the Al atoms and some impurities in the ZA, as shown in Table 1. As a result, ZAA exhibited the highest Si/Al ratio and lowest surface area. On the contrary, the alkaline treatment on the ZA caused an increase in the surface area. Eventually, the ZAB possessed the lowest average pore diameter among others. NaOH treatment might eliminate the impurities in the zeolite channel while preserving the zeolite network, as indicated by the slight modification in the Si/Al ratio (see Table 1). It can also be explained that both aluminum and silicon atoms are extracted during the NaOH treatment [34].
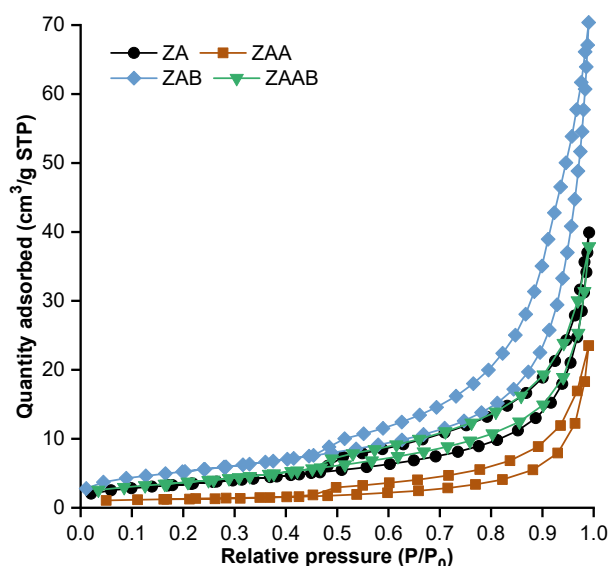
Fig 3. Nitrogen adsorption/desorption isotherms of natural zeolite (ZA) after being subjected to acetic acid and alkaline treatment

Table 2. Surface parameters of catalysts

Catalyst	Surface area (m² g⁻¹)	Total pore volume (cm³ g⁻¹)[b]	D (nm)[b]
ZA	12.542	0.06	19.24
ZAA	4.058	0.04	35.71
ZAB	19.144	0.11	17.02
ZAAB	13.144	0.06	22.70

[a]Surface area determined by using BET theory. [b]Total pore volume (at P/P₀ = 0.99), and average pore volume determined by using BJH theory
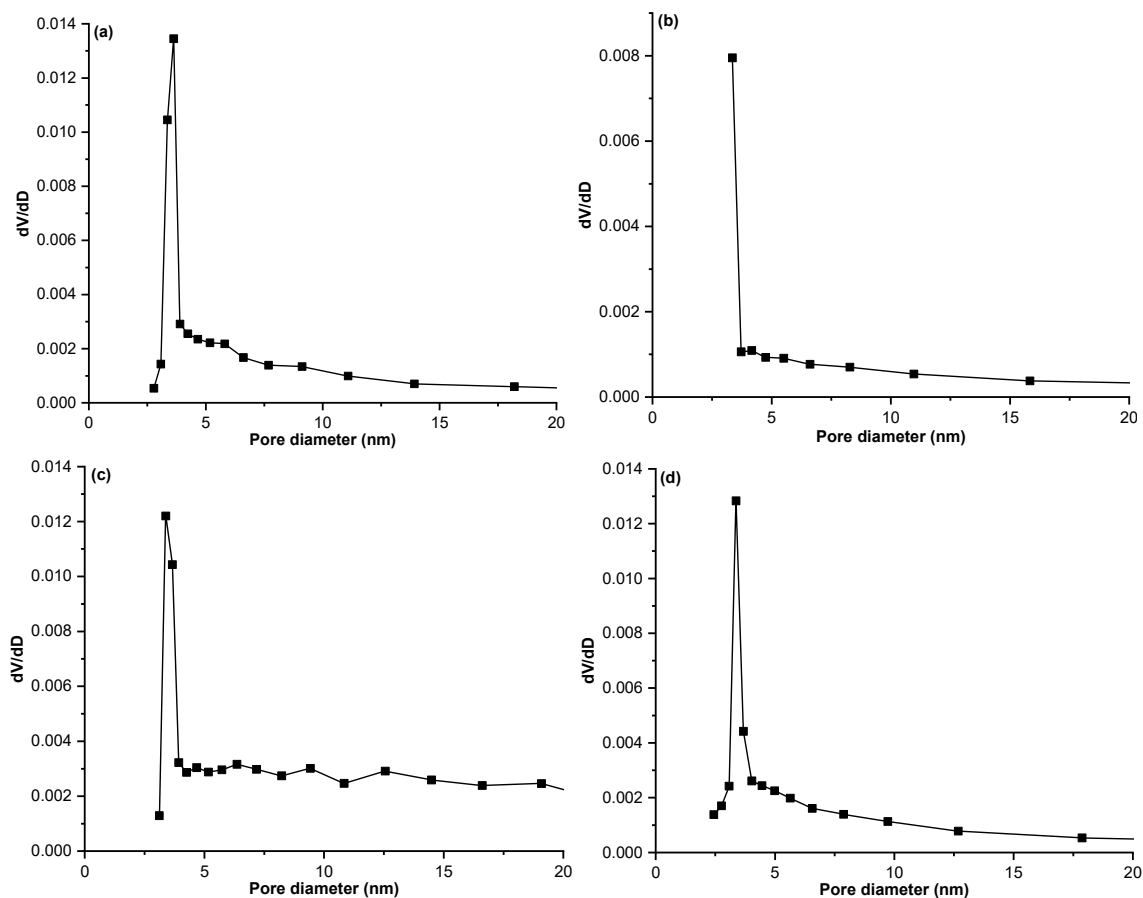
Fig 4. Pore size distribution of (a) ZA, (b) ZAB, (c) ZAA, and (d) ZAAB

It is well known that a catalyst possessing a high surface area is desirable to obtain high catalytic activity due to the accessibility of the active catalytic site. There is a limited number of reports on the application of acetic acid in acid treatment. Chung [22] reported that acetic acid treatment on the Mordenite increased the surface area and the alkylation reaction of cumene and 2-propanol. Moreover, it also overcomes the diffusion limitation of the Mordenite as a catalyst. Yusniyanti et al. [35] revealed that a combination of acetic acid and NaOH treatment on Mordenite caused the increment of its catalytic activity towards the hydrotreatment of bio-oil obtained from cellulose. Both report the positive effect on the application of zeolite catalyst after the acid or acid-alkaline treatment. As revealed in Table 1 and 2, the Si/Al ratio and surface area of zeolite changed upon the acid and the combination of acid-alkaline treatment. Therefore, treated zeolite is expected to exhibit better catalytic performance than natural zeolite.

Catalytic Activity and Selectivity of ZA, ZAA, ZAB, and ZAAB Catalysts in Hydrotreatment of Castor Oil

Castor oil has high linoleic acid content and the potential to be used as feed to obtain biofuel. The hydrotreatment process is needed to turn castor oil into valuable biofuel. Here, the prepared catalysts (ZA, ZAA, ZAB, and ZAAB) were tested on the hydrotreatment of castor oil to evaluate the effect of the acetic acid, and NaOH treatment on the ZA and the results are shown in Table 3. The liquid product from the hydrocracking process was analyzed using GC-MS to determine the plausible compound (Fig. S1 and Table S1). The GC-MS results showed a small distribution of hydrocarbons from the radical cracking mechanism, and the liquid product still contained a lot of oxygenated compounds. Table 3 shows that all the catalysts exhibit high conversion of castor oil, around 98–99%. The aspect of choosing the best catalyst is the liquid production percentage.

Table 3. Products distribution of hydrotreatment of castor oil

Catalyst	Conv. (wt.%)	Gas (wt.%)	Liquid fraction (wt.%)				Coke (wt.%)	Residue (wt.%)
			Gasoline	Diesel	Others	Total		
ZA	99.7	45.0	11.6	1.5	40.7	53.9	0.8	0.3
ZAB	97.8	41.4	19.5	2.9	32.6	55.1	1.3	2.2
ZAA	99.8	58.0	13.1	6.8	21.6	41.6	0.2	0.2
ZAAB	98.6	42.0	18.6	1.0	35.1	54.8	1.8	1.4

As presented in Table 3, the catalysts show different performances in terms of liquid production. The acetic acid treatment on ZA (ZAA) caused a decrease in catalytic activity, which exhibited the most inadequate liquid production (41.6%), suggesting due to a decrease in the surface area after the acid treatment. Although the ZAA catalyst that only underwent acid treatment exhibited the lowest catalytic activity due to the low surface area, the ZAA catalyst produces the least amount of coke and high selectivity to the diesel fraction contributing to its big pore diameter. It indicated that acid treatment on the ZA has a positive effect on lowering the coke production in the catalyst, which could slow down the deactivation of the catalyst. Further treatment of the ZAA with the NaOH (ZAAB) recovers the surface area and catalytic activity. The liquid production increased from 41.6 to 54.8%, with 18.6% selectivity towards the gasoline fraction.

Interestingly, the ZAB catalyst, which resulted from the NaOH treatment on ZA, showed the highest liquid production (55.1%) with 19.5% selectivity towards the gasoline fraction, contributing to increased catalyst surface area. Because active sites were created on the surface of the catalysts, increasing the surface area of the catalysts increases the availability of active sites, resulting in increased catalytic activity. As shown in Table 2, the ZAB exhibits the highest surface among others. The surface area of the catalyst is in the order (from the lowest to the highest): ZAA < ZAAB < ZA < ZAB, and the catalytic activity is in the order: ZAA < ZA < ZAAB < ZAB.

Correlation between Specific Surface Area towards the Activity of the Catalysts

The correlation between the specific surface area of catalysts and the number of liquid products produced is shown in Fig. 5. The amount of liquid product made was also used to determine the catalyst's activity. Fig. 5 offered
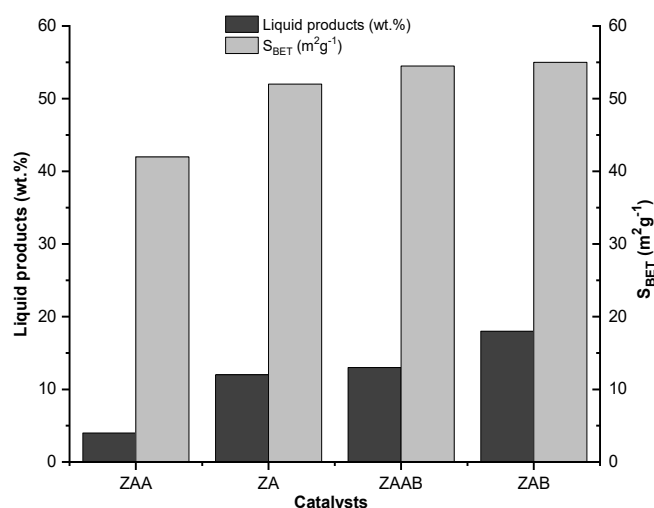
Fig 5. Correlation between the specific surface area of catalysts and the amount of liquid product

that the number of liquid products produced increases as the specific surface area of the catalyst increases. Increases in a catalyst's specific surface area can improve active sites' availability. Catalytic reactions rely heavily on active sites [36]. The ZAB exhibited the highest catalytic activity, attributed to its large specific surface area. Due to its low specific surface area, the ZAA showed the most insufficient catalytic activity. This conclusion is consistent with the research from [37], which indicates that a catalyst with a high specific surface area has a greater chance of exhibiting good catalytic activity during the hydrocracking process.

■ CONCLUSION

In this study, the preparation of heterogeneous catalysts has successfully been carried out. The acetic acid and sodium hydroxide treatment was treated on Wonosari natural zeolite and denoted as ZAA, ZAB, and ZAAB. The acid treatment towards zeolite increased Si/Al ratio from 7.30 to 7.85, respectively. Sodium

hydroxide treatment decreased Si/Al ratio from 7.30 to 7.26 and after acid-sodium hydroxide treatment from 7.85 to 7.61, respectively. The ZA, ZAB, ZAA, and ZAAB catalysts produced liquid products of 53.9, 55.1, 41.6, and 54.8 wt.%, respectively. The ZAB had the highest liquid product with selectivity towards hydrocarbon compounds of 22.4 wt.%. The higher specific surface area increased the activity and selectivity of the catalyst towards liquid production and hydrocarbon compounds in the hydrotreatment process of castor oil. The ZAB catalyst showed the highest surface area.

■ ACKNOWLEDGMENTS

■ AUTHOR CONTRIBUTIONS

Lailatul Rahmi conducted the research and wrote the manuscript, Wega Trisunaryanti proposed the research topic and revised the manuscript, Triyono and Iip Izul Falah revised the manuscript.

■ REFERENCES

[1] Anuar, M.R., and Abdullah, A.Z., 2016, Challenges in biodiesel industry with regards to feedstock, environmental, social and sustainability issues: A critical review, *Renewable Sustainable Energy Rev.*, 58, 208–223.

[2] Rabie, A.M., Shaban, M., Abukhadra, M.R., Hosny, R., Ahmed, S.A., and Negm, N.A., 2019, Diatomite supported by CaO/MgO nanocomposite as heterogeneous catalyst for biodiesel production from waste cooking oil, *J. Mol. Liq.*, 279, 224–231.

[3] Ajala, O.E., Aberuagba, F., and Odetoye, T.E., 2015, Biodiesel: Sustainable energy replacement to petroleum-based diesel fuel – A review, *ChemBioEng Rev.*, 2 (3), 145–156.

[4] Zhang, Q., Wang, T., Xu, T., Zhang, Q., and Ma, L., 2014, Production of liquid alkanes by controlling reactivity of sorbitol hydrogenation with a Ni/HZSM-5 catalyst in water, *Energy Convers. Manage.*, 77, 262–268.

[5] Atabani, A.E., Silitonga, A.S., Ong, H.C., Mahlia, T.M.I., Masjuki, H.H., Badruddin, I.A., and Fayaz, H., 2013, Non-edible vegetable oils: A critical evaluation of oil extraction fatty acid compositions, biodiesel productions, characteristic, engine performance, and emissions production and refining technologies, *Renewable Sustainable Energy Rev.*, 18, 211–245.

[6] Kamel, D.A., Farag, H.A., Amin, N.K., Zatout, A.A., and Ali, R.M., 2018, Smart utilization of jatropha (*Jatropha curcas* Linnaeus) seeds for biodiesel production: Optimization and mechanism, *Ind. Crops Prod.*, 111, 407–413.

[7] Vorontsov, A.V., Valdés, H., and Smirniotis, P.G., 2019, Design of active sites in zeolite catalysts using modern semiempirical methods: The case of mordenite, *Comput. Theor. Chem.*, 1166, 112572.

[8] Alver, B.E., and Esenli, F., 2017, Acid treated mordenites as adsorbents of C_2H_4 and H_2 gases, *Microporous Mesoporous Mater.*, 244, 67–73.

[9] Sousa, L.V., Silva, A.O.S., Silva, B.J.B., Quintela, P.H.L., Barbosa, C.B.M., Fréty, R., and Pacheco, J.G.A., 2018, Preparation of zeolite P by desilication and recrystallization of zeolites ZSM-22 and ZSM-35, *Mater. Lett.*, 217, 259–262.

[10] Ahmad, M., Farhana, R., Raman, A.A.A., and Bhargava, S.K., 2016, Synthesis and activity evaluation of heterometallic nano oxides integrated ZSM-5 catalysts for palm oil cracking to produce biogasoline, *Energy Convers. Manage.*, 119, 352–360.

[11] Zhao, X., Wei, L., Julson, J., Gu, Z., and Cao, Y., 2015, Catalytic cracking of inedible camelina oils to hydrocarbon fuels over bifunctional Zn/ZSM-5 catalysts, *Korean J. Chem. Eng.*, 32 (8), 1528–1541.

[12] Žibert, J., Cedilnik, J., and Pražnikar, J., 2016, Particulate matter (PM10) patterns in Europe: An exploratory data analysis using non-negative matrix factorization, *Atmos. Environ.*, 132, 217–228.

[13] Procházka, P., and Hönig, V., 2018, Economic analysis of diesel-fuel replacement by crude palm oil in Indonesian power plants, *Energies*, 11 (3), 504.

[14] De, S., and Luque, R., 2014, Upgrading of waste oils into transportation fuels using hydrotreating technologies, *Biofuel Res. J.*, 1 (4), 107–109.

[15] Zarchin, R., Rabaev, M., Vidruk-Nehemya, R., Landau, M.V., and Herskowitz, M., 2015, Hydroprocessing of soybean oil on nickel-phosphide supported catalysts, *Fuel*, 139, 684–691.

[16] Bezergianni, S., Dimitriadis, A., and Meletidis, G., 2014, Effectiveness of CoMo and NiMo catalysts on co-hydroprocessing of heavy atmospheric gas oil-waste cooking oil mixtures, *Fuel*, 125, 129–136.

[17] Kristiani, A., Sudiyarmanto, S., Aulia, F., Hidayati, L.N., and Abimanyu, H., 2017, Metal supported on natural zeolite as catalysts for conversion of ethanol to gasoline, *MATEC Web Conf.*, 101, 01001.

[18] Sriningsih, W., Saerodji, M.G., Trisunaryanti, W., Triyono, T., Armunanto, R., and Falah, I.I., 2014, Fuel production from LDPE plastic waste over natural zeolite supported Ni, Ni-Mo, Co and Co-Mo Metals, *Procedia Environ. Sci.*, 20, 215–224.

[19] Sun, Q., Wang, N., and Yu, J., 2021, Advances in catalytic of zeolite-supported metal catalysts, *Adv. Matter.*, 33 (51), 2104442.

[20] Trisunaryanti, W., Wijaya, K., Suryani, D., and Chasanah, U., 2021, "The Effect of HNO_3 and/or NaOH Treatments on Characteristics of Mordenite" in *Advances in Geopolymer-Zeolite Composites - Synthesis and Characterization*, Eds. Vizureanu, P., and Krivenko, P., IntechOpen, Rijeka, 83–89.

[21] Anggoro, D.D., Oktavianty, H., Sasongko, S.B., and Buchori, L., 2020, Effect of dealumination on the acidity of zeolite Y and the yield of glycerol mono stearate (GMS), *Chemosphere*, 257, 127012.

[22] Chung, K.H., 2008, Dealumination of mordenites with acetic acid and their catalytic activity in the alkylation of cumene, *Microporous Mesoporous Mater.*, 111 (1-3), 544–550.

[23] Muttaqii, M., Birawidha, C.D., Isnugroho, K., Amin, M., Hendro, Y., Istiqomah, A., and Dewangga, D., 2019, Pengaruh aktivasi secara kimia menggunakan larutan asam dan basa terhadap karakteristik zeolit alam, *JRTI*, 13 (2), 266–271.

[24] Bertrand-Drira, C., Cheng, X.W., Cacciaguerra, T., Trens, P., Melinte, G., Ersen, O., Minoux, D., Finiels, A., Fajula, F., and Gerardin, C., 2015, Mesoporous mordenites obtained by desilication: Mechanistic considerations and evaluation in catalytic oligomerization of pentene, *Microporous Mesoporous Mater.*, 213, 142–149.

[25] Gea, S., Haryono, A., Andriayani, A., Sihombing, J.L., Pulungan, A.N., Nasution, T., Rahayu, R., and Hutapea, A.Y., 2020, The effect of chemical activation using base solution with various concentrations towards sarulla natural zeolite, *Elkawnie*, 6 (1), 85–95.

[26] Ates, A., 2018, Effect of alkali-treatment on the characteristics of natural zeolites with different compositions, *J. Colloid Interface Sci.*, 523, 266–281.

[27] Triyono, T., Trisunaryanti, W., and Yusniyanti, F., 2020, Sonicated-assisted acid treatment of mordenite using acetic acid, *Key Eng. Mater.*, 840, 520–525.

[28] Tišler, Z., Hrachovcová, K., Svobodová, E., Šafář, J., and Pelíšková, L., 2019, Acid and thermal treatment of alkali-activated zeolite foams, *Minerals*, 9 (12), 719.

[29] Wei, Y., Parmenrier, T.E., de Jong, K.P., and Zečević, J., 2015, Tailoring and visualizing the pore architecture of hierarchical zeolites, *Chem. Soc. Rev.*, 44 (20), 7234–7235.

[30] Wijaya, K., Baobalabuana, G., Trisunaryanti, W., and Syoufian, A., 2013, Hydrotreatment of palm oil into biogasoline catalyzed by Cr/natural zeolite, *Asian J. Chem.*, 25 (16), 8981–8986.

[31] Trisunaryanti, W., Triyono, T., Falah, I.I., Widyawati, D., and Yusniyanti, F., 2022, The effect of oxalic acid and NaOH treatments on the character of Wonosari natural zeolite as Ni, Cu, and Zn metal support catalyst for hydrocracking of castor oil, *Biomass Convers. Biorefin.*, 2022, s13399-022-02779-5.

[32] Kurniawan, T., Muraza, O., Bakare, I.A., Sanhoob, M.A., and Al-Amer, A.M., 2018, Isomerization of

n-butane over cost-effective mordenite catalyst frabicated via recrystallization of natural zeolite, *Ind. Eng. Chem. Res.*, 57 (6), 1894–1902.

[33] Ramesh, K., Reddy, K.S., Rashmi, I., and Biswas, A.K., 2014, Porosity distribution, surface area and morphology of synthetic potassium zeolites: A SEM and N_2 adsorption study, *Commun. Soil Sci. Plant Anal.*, 45 (16), 2171–2181.

[34] Nurliati, G., Krisnandi, Y.K., Sihombing, R., and Salimin, Z., 2015, Studies of modification of zeolite by tandem acid-base treatments and its adsorptions performance towards thorium, *Atom Indonesia*, 41 (2), 87–95.

[35] Yusniyanti, F., Trisunaryanti, W., and Triyono, T.,

2021, Acid-alkaline treatment of mordenite and its catalytic activity in the hydrotreatment of bio-oil, *Indones. J. Chem.*, 21 (1), 37–45.

[36] Bernard, P., Stelmachowski, P., Broś, P., Makowski, W., and Kotarba, A., 2021, Demonstration of the influence of specific surface area on reaction rate in heterogeneous catalysis, *J. Chem. Educ.*, 98 (3), 935–940.

[37] Trisunaryanti, W., Triyono, T., Purwono, S., Purwanti, S.A., and Sumbogo, S.D., 2021, Synthesis of mesoporous carbon from merbau sawdust as a nickel metal catalyst support for castor oil hydrocracking, *Bull. Chem. React. Eng. Catal.*, 17 (1), 216–224.